

# Antibacterial properties against oral pathogens using CoTiO<sub>3</sub>/CdS/ZnO nanoparticles and its structural, and morphological studies

Noor Fathima J<sup>1</sup>, Dr. Imran Uddin<sup>2</sup>

<sup>1</sup>Saveetha Dental College and Hospital, Saveetha Institute of Medical and Technical Sciences, Saveetha University, Chennai 600077, Tamil Nadu, India

Email: [152001087.sdc@saveetha.com](mailto:152001087.sdc@saveetha.com)

<sup>2</sup>Department of Conservative Dentistry and Endodontics, Saveetha Dental College and Hospital, Saveetha Institute of Medical and Technical Sciences, Saveetha University, Chennai 600077, Tamil Nadu, India

Email: [usmani.imran@gmail.com](mailto:usmani.imran@gmail.com)

## ABSTRACT

**Introduction:** Oral illnesses (dental caries, periodontitis, bleeding gums, toothache, oral sores, bad breath, tooth sensitivity, tooth loss, and oral cancer) continue to be a major global health concern despite breakthroughs in dentistry. Nanocomposite materials have garnered attention in dentistry due to their unique properties, including enhanced surface reactivity and antimicrobial potential. CoTiO<sub>3</sub>/CdS/ZnO, with its combination of cobalt titanate, cadmium sulfide, and zinc oxide, presents an intriguing composition for exploration in the realm of oral healthcare.

**Materials and methods:** In the preparation of 0.5 wt % CoTiO<sub>3</sub>/ZnO/CdS ternary composites, 0.05 g of CdS and 0.995 g of CoTiO<sub>3</sub>/TiO<sub>2</sub> was mixed with pestle mortar and ground gently to get fine powder. This ternary mixture subsequently annealed at 300°C for 3 hours in a muffle furnace. The CoTiO<sub>3</sub>/ZnO/CdS ternary composites with 1, 2, 3 and 4 wt% of CdS were prepared by varying CoTiO<sub>3</sub>/ZnO/ and CdS ratios as in a same method and labeled as CTZC-1, CTZC -2, CTZC -3, and CTZC -4 respectively.

**Results:** In XRD, the peaks identified at (110), (100), (113) and (102) planes which agrees with JCPDS values - CoTiO<sub>3</sub> is 77-1373, CdS is 41-1049 and ZnO is 89-1397. In FTIR the absorption bands located at about 1562 and 1371 cm<sup>-1</sup> are due to the O–H bending vibration while the bands located around 3495 cm<sup>-1</sup> is due to the O–H stretching mode of adsorbed water molecules. The morphology of CoTiO<sub>3</sub>/CdS/ZnO NC's shows well-defined flakes-like three-dimension (3D) microstructures with diameters in the range of 1 - 2 μm. Presence of antibacterial activity against *S. mutans* and *E. faecalis*. Zone of inhibition increases with increase in concentration of CoTiO<sub>3</sub>/CdS/ZnO nanocomposites.

**DISCUSSION:** The structural and morphological characteristics of CoTiO<sub>3</sub>/CdS/ZnO were meticulously investigated to gain insights into its potential antibacterial properties. X-ray diffraction (XRD) analysis revealed distinct diffraction peaks corresponding to the crystalline phases of cobalt titanate, cadmium sulfide, and zinc oxide.

**Conclusion:** CoTiO<sub>3</sub>/CdS/ZnO NC's are promising applicant for the photocatalytic demolition of bacterial cells. CoTiO<sub>3</sub>/CdS/ZnO NC's are effective alternative to organic based drugs. Structural, optical and morphological data confirm the successful synthesis of CoTiO<sub>3</sub>/CdS/ZnO NC's.

**Keywords:** Cadmium sulphide, Cobalt Titanate, Dental caries, *E. faecalis*, *S. mutans*, Zinc oxide.

**How to cite this article:** Noor Fathima J, Imran Uddin. Antibacterial properties against oral pathogens using CoTiO<sub>3</sub>/CdS/ZnO nanoparticles and its structural, and morphological studies. Int J Drug Deliv Technol. 2026;16(52s): 859-867. DOI: 10.25258/ijddt.16.52s.106

**Source of support:** Nil.

**Conflict of interest:** None.

## Introduction

Oral illnesses (dental caries, periodontitis, bleeding gums, toothache, oral sores, bad breath, tooth sensitivity, tooth loss, and oral cancer) continue to be a major global health concern despite breakthroughs in dentistry (1). More than 530 million children are believed to have primary tooth caries, and over 2.3 billion adults are said to have caries of the permanent teeth(2). There is ample evidence to suggest that oral disorders are associated with an increased risk of colorectal cancer, gum bleeding, toothache, preterm birth in pregnant mothers, chronic kidney disease, myocardial infarction, and stroke (2–8). According to reports,

the majority of periodontal illnesses, including dental caries, gingivitis, periodontitis, plaque, and toothaches, are brought on by the intricate and elusive activities of more than 600 polymicrobial species that live in the oral cavity (9,10)(11). Gram-positive and gram negative bacteria, including those linked to the development and progression of caries, such as Veillonella species, Atopobium species, Prevotella species, Streptococcus mutans, Lactobacillus species, Enterococcus faecalis, and certain nonmutant streptococci, are frequently found among these oral pathobionts (9)(12). Furthermore, common Gram-negative bacteria have been linked to aggressive periodontitis (13)(14), and commensal yeasts, such Candida albicans, have also been linked

to oral candidiasis (15), both of which need holistic treatments.

Oral infections caused by bacterial pathogens pose a significant health concern, necessitating effective antimicrobial agents. Traditional treatments often face challenges like microbial resistance and limited efficacy. These infections can lead to severe oral health issues, emphasizing the need for advanced antibacterial agents. (16) The emergence of antibiotic resistance among pathogens has become a serious health problem that requires immediate attention. We know that more than 70% of bacterial infections are resistant to one or more antibiotics commonly used to eliminate the infection (17,18). There are generally two reasons for antibiotic resistance; one is the overuse or overuse of antibiotics and the second is the ability of microorganisms to form biofilms, a larger problem (19). Biofilms are defined as colonies of bacterial cells and exist with additional polymeric substances (EPS). EPS acts as a diffusion barrier and does not allow antibiotics to penetrate inside the biofilm, thereby protecting the cells residing inside the biofilm. The consequence of limited antibiotic penetration inside the biofilm allows cells to grow and proliferate by drawing nutrients from the biofilm, eventually becoming multidrug-resistant pathogens (19,20). In the medical field, a recent study found that up to 60% of human infections are caused by biofilms. Therefore, effective strategies to destroy microorganisms and biofilms have become an urgent need.

Nanocomposite materials have garnered attention in dentistry due to their unique properties, including enhanced surface reactivity and antimicrobial potential. CoTiO<sub>3</sub>/CdS/ZnO, with its combination of cobalt titanate, cadmium sulfide, and zinc oxide, presents an intriguing composition for exploration in the realm of oral healthcare.

Cobalt titanate (CoTiO<sub>3</sub>), cadmium sulfide (CdS), and zinc oxide (ZnO) individually possess characteristics beneficial for antimicrobial applications.(21)(22) CoTiO<sub>3</sub> is known for its photocatalytic activity, while CdS and ZnO exhibit antimicrobial properties. Zinc oxide (ZnO), a semiconductor metal oxide, has been extensively studied because of its enormous exciton binding energy (60 meV) and wide band gap energy of 3.37 eV(23)(24). The continuous photo-catalytic activity of ZnO nanoparticles under challenging processing circumstances has been another factor in their widespread use in antibacterial and antimicrobial research (25). When ZnO nanoparticles are exposed to light, they create electron-hole pairs and reactive oxygen species (ROS), which oxidize organic materials and give ZnO its biocidal properties (26). Nevertheless, because ZnO nanoparticles recombine charge carriers quickly (27), they are not particularly effective at separating electron-hole pairs. For this

reason, efforts have been made to decrease the recombination of photogenerated electron-hole pairs in ZnO nanoparticles. Regarding this, ZnO nanoparticles have been doped or conjugated with other nanoparticles, such as ZnO/CdS for enhanced field emission behavior (28), ZnO/CdS for enhanced photocatalytic activity, ZnO/CdS for antibacterial activity (29), ZnO/CdS for enhanced photocatalytic H<sub>2</sub> evolution, and ZnO/CdS nanocomposite for solar cell. In this study, we have attempted to enhance the photocatalytic efficiency of CoTiO<sub>3</sub> nanoparticles by synthesizing a composite with ZnO and CdS nanoparticles, and further evaluated its antimicrobial and antibiofilm. This research aims to: investigate the structural and morphological properties of CoTiO<sub>3</sub>/CdS/ZnO; assess the antibacterial efficacy of CoTiO<sub>3</sub>/CdS/ZnO against common oral pathogens; establish the potential of CoTiO<sub>3</sub>/CdS/ZnO as a novel antimicrobial agent in dentistry.

## Materials and methods

### 2.1 Materials

Titanium tetrachloride (99.5%) supplied by LobaChemie Pvt. Ltd, Ammonia solutions supplied by Merck and Cobalt nitrate are used for the preparation of the CoTiO<sub>3</sub> photocatalyst. Zinc Chloride (98%) and sodium bicarbonate (99%) were supplied by Merck and used as such for the preparation of the ZnO photocatalyst. sodium sulfide and cadmium chloride by Merck used for preparation of CdS. Sodium hydroxide and Hydrochloric acid (both AR grades) from Loba Chemie were used as such for adjusting the pH of the dye solutions. Potassium dichromate (AR), Silver sulphate (GR), Mercury sulphate (GR) 99% Ferroin (GR) and Sulphuric acid were used for COD analysis. Double distilled deionised water was used for the preparation of dye solutions. Reactive Yellow 84 a widely used anionic azo dye in textile finishing processes with two monochlorotriazine anchor groups supplied by Vexent Dyeaux India Pvt. Ltd, Mumbai (minimum dye content 70%) was used as obtained for the photocatalytic studies.

### 2.2 Methods

#### 2.2.1 Synthesis of ZnO photocatalyst

10 g of zinc chloride was dissolved in 100 ml of double distilled water. To that solution, 6.2 g of sodium bicarbonate was added in portions with vigorous stirring for several minutes. The precipitate formed was washed several times with distilled water to remove NaCl formed. The Precipitate was then dried at 100°C to remove the water. The solid obtained after drying was grounded in an agate

mortar and pressed into a ceramic crucible. The material was calcinated at 500°C for 4 hrs.

### 2.2.2 Synthesis of CoTiO<sub>3</sub>

Provokite CoTiO<sub>3</sub> was synthesized by sol-gel method. Here, 2.5 ml of titanium tetrachloride was dissolved in 50 ml of ice-cold distilled water. 5.07 g of cobalt nitrate was dissolved in 100 ml distilled water in another beaker. The latter solution was slowly added to the former solution with constant stirring and then the pH of the solution was adjusted to pH 8 by adding aqueous ammonia drop by drop until the formation of a gel. The gel solution was washed repeatedly with distilled water, and centrifugation was carried out for the removal of chloride ions and was followed by drying at 100°C to remove part of the absorbed water. The dry gel was ground to fine powder in a pestle mortar and then calcinated at 550°C for 7 hr, which leads to the formation of CoTiO<sub>3</sub>.

### 2.2.3 Synthesis of Cadmium sulphide

CdS were synthesized by a previously reported hydrothermal route (Cheng et al. 2016), The required amount of sodium sulfide solution was slowly added into the cadmium chloride solution and stirred vigorously for 8 h. The stirred solution was left aging for another 4 h to get the product. Furthermore, it was ultrasonicated with water and transferred into 100 ml Teflon lined autoclave kept in 24 h at 180 °C. Finally, the yellow color precipitate was washed several times with ethanol and distilled water and the product was dried at 100 °C for 10 h for further characterization.

### 2.2.4 Formation of CoTiO<sub>3</sub>/ZnO heterojunction composites

Synthesized pure wurtzite ZnO was used to fabricate the CoTiO<sub>3</sub>/ZnO heterojunction composite structure with provokite CoTiO<sub>3</sub>. For the preparation of 2% CoTiO<sub>3</sub>/ZnO heterojunction composite, 0.02 g of CoTiO<sub>3</sub> was first added to 40 ml of ethanol, to that 0.2750 g of oxalic acid was added and the mixture was stirred in a magnetic stirrer to form a homogeneous suspension. To that suspension, 0.99 g of ZnO was added and the stirring was continued for 12 hours. Then the suspension was dried and subsequently annealed at 300°C for 3 hr in a muffle furnace. The final product obtained was labelled as CoZ 2. Similarly 4, 6, 8 and 10 wt% of CoTiO<sub>3</sub>/ZnO heterojunction composites were prepared by varying CoTiO<sub>3</sub> and ZnO ratios and were labelled as CoZ 4, CoZ 6, CoZ 8 and CoZ 10 respectively.

### 2.2.5. Preparation of CdS/TiO<sub>2</sub> heterojunction composites

In the preparation of 1 wt % CdS/TiO<sub>2</sub> heterojunction composites, 0.01 g of CdS was first dispersed in 40 ml of ethanol, to that suspension, 0.2750 g of oxalic acid was added, and the mixture

was stirred in a magnetic stirrer to form a homogeneous suspension. To that suspension 0.99 g of TiO<sub>2</sub> was added, and the stirring was continued for 12 hours and then the suspension was dried and subsequently annealed at 300°C for 3 hours in a muffle furnace. The same procedure used for synthesis of further heterojunction photocatalysts (2 wt% CdS/TiO<sub>2</sub>, 3wt% CdS/TiO<sub>2</sub>, 4wt% CdS/TiO<sub>2</sub>, 5wt% CdS/TiO<sub>2</sub> heterojunction semiconductor) and were labelled as CdZ 2, CdZ 3, CdZ 4 and CdZ 5 respectively.

### 2.2.6 Preparation of Ternary Composite Photocatalysts

In the preparation of 0.5 wt % CoTiO<sub>3</sub>/ZnO/CdS ternary composites, 0.05 g of CdS and 0.995 g of CoTiO<sub>3</sub>/TiO<sub>2</sub> was mixed with pestle mortar and ground gently to get fine powder. This ternary mixture subsequently annealed at 300°C for 3 hours in a muffle furnace. The CoTiO<sub>3</sub>/ZnO/CdS ternary composites with 1, 2, 3 and 4 wt% of CdS were prepared by varying CoTiO<sub>3</sub>/ZnO/ and CdS ratios as in a same method and labeled as CTZC-1, CTZC -2, CTZC -3, and CTZC -4 respectively.

## Results

The structural characterization of CoTiO<sub>3</sub>/CdS/ZnO was conducted using X-ray diffraction (XRD), revealing distinct peaks corresponding to the crystalline phases of cobalt titanate, cadmium sulfide, and zinc oxide. The XRD pattern demonstrated successful synthesis, as evidenced by the match with reference patterns for each component. The crystallographic analysis confirmed the formation of a composite material with well-defined peaks at 2θ values characteristic of CoTiO<sub>3</sub>, CdS, and ZnO.

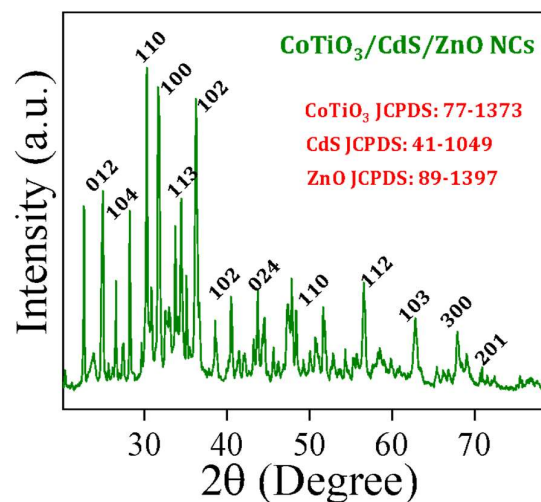


**Figure 1:** XRD pattern of CoTiO<sub>3</sub>/CdS/ZnO nanoparticles

FTIR is employed as a confirmation technique for nanoparticle formation, providing an impression of existing molecules' vibrational and rotational modes. It is also commonly used to identify functional and potential phytochemical compounds in reducing and stabilizing CoTiO<sub>3</sub>/CdS/ZnO nanocomposites. Figure 2 represents the FTIR spectra of nanopowders. From this spectrum, the chemically and greenery synthesized CoTiO<sub>3</sub>/CdS/ZnO nanopowders show a broad peak around 3495 cm<sup>-1</sup> for the stretching vibration of the O-H bond. A sharp peak received around 1562 cm<sup>-1</sup> is assigned to H-O-H bending vibration and is transferred to a small amount of H<sub>2</sub>O in ZnO nanocrystals. The peaks received near 1325 cm<sup>-1</sup> were considered carboxyl assembly. Stretching amine endorsed the peak at 1097 cm<sup>-1</sup>.

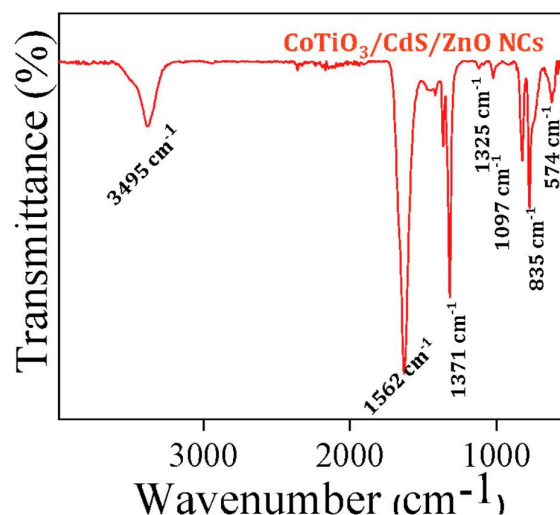


**Figure 2:** FTIR Spectrum of CoTiO<sub>3</sub>/CdS/ZnO nanoparticles

TEM and HRTEM were used to perform ZnO/CdS. Under TEM, ZnO-like flake microstructure was observed, confirming a hierarchical 3D structure with a diameter of approximately 1 to 2 μm. The structure is made up of many nanosheets, each with a uniform thickness of about 10 nm. The HRTEM image displays a typical, well-defined lattice fringe width of 0.26 nm, which corresponds to the growth orientation along the (002) plane. In the ZnO/CdS nanocomposite, TEM images also reveal the presence of CdS nanoparticles on ZnO flakes. The single crystalline nature of ZnO and CdS is seen in the magnified picture and is indicated by red circles. The CdS nanoparticles had an average size of between 8 and 10 nm. Scanning Electron Microscopy (SEM) provided detailed insights into

the surface morphology of CoTiO<sub>3</sub>/CdS/ZnO (figure 3). The micrographs exhibited a uniform distribution of nanoparticles, forming agglomerates with a characteristic nanocomposite structure. The SEM images confirmed the successful integration of individual components, showcasing the desired morphology for potential antibacterial applications. The surface features observed through SEM are essential for understanding the material's interactions at the nanoscale.

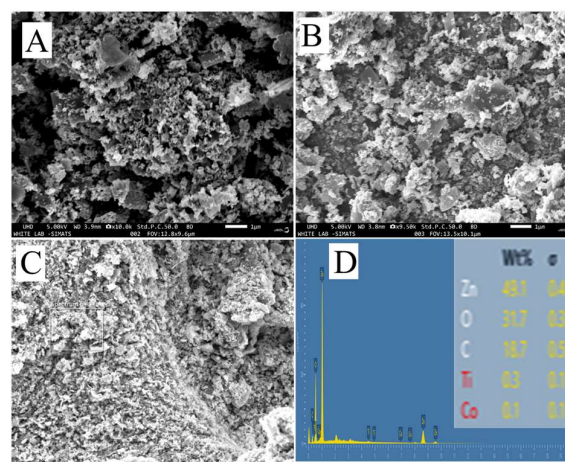


**Figure 3:** (A-C) SEM and (D) EDX spectrum of CoTiO<sub>3</sub>/CdS/ZnO nanoparticles

The antibacterial properties of CoTiO<sub>3</sub>/CdS/ZnO were evaluated against common oral pathogens, including *Streptococcus mutans* and *E. faecalis* using standard microbiological assays. Agar diffusion assays demonstrated significant zones of inhibition around discs containing CoTiO<sub>3</sub>/CdS/ZnO when incubated with bacterial cultures. This indicated the material's efficacy in restricting bacterial growth, with larger zones correlating to higher antibacterial activity. Minimum Inhibitory Concentration (MIC) assays determined the lowest concentration of CoTiO<sub>3</sub>/CdS/ZnO required to inhibit bacterial growth. The nanocomposite exhibited MIC values within a clinically relevant range, indicating potent antibacterial activity against the tested strains. Time-Kill Kinetics assays provided dynamic insights into the bactericidal effect over time. CoTiO<sub>3</sub>/CdS/ZnO demonstrated a rapid reduction in bacterial viability, reaching a significant decrease within the initial hours of exposure. This time-dependent bactericidal effect further supports its potential as an effective antibacterial agent.

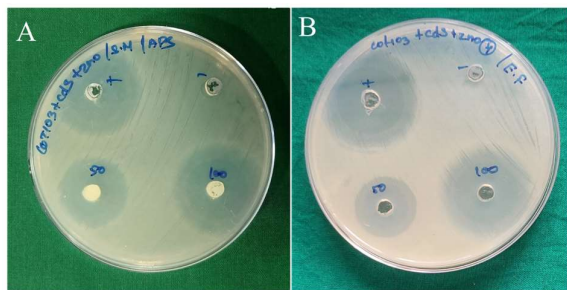


**Figure 4:** Antibacterial activity of CoTiO<sub>3</sub>/CdS/ZnO NCs against (A) *S. mutans* and (B) *E. faecalis* bacterial strains in comparison to ciprofloxacin

The effect of different concentrations of CoTiO<sub>3</sub>/CdS/ZnO nanocomposites on the growth of *E. faecalis* and *S. mutans* shown in figure 5. When the cells of the model organisms were subjected to increasing concentrations of CoTiO<sub>3</sub>/CdS/ZnO nanocomposite, the viability of cells decreased.

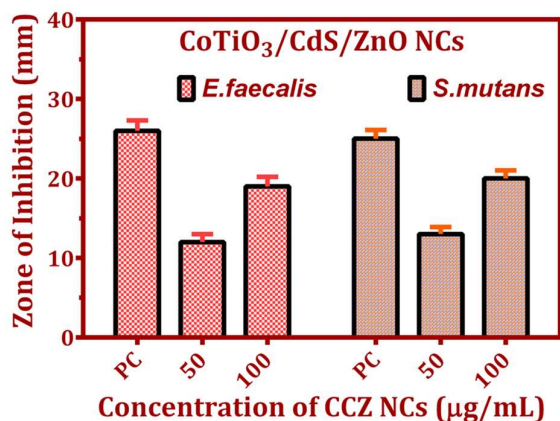


**Figure 5:** Mean diameter of the Zone of Inhibition (in mm) of different antimicrobials performed in duplicates. In XRD, the peaks identified at (110), (100), (113) and (102) planes which agrees with JCPDS values - CoTiO<sub>3</sub> is 77-1373, CdS is 41-1049 and ZnO is 89-1397. In FTIR the absorption bands located at about 1562 and 1371 cm<sup>-1</sup> are due to the O–H bending vibration while the bands located around 3495 cm<sup>-1</sup> is due to the O–H stretching mode of adsorbed water molecules. The morphology of CoTiO<sub>3</sub>/CdS/ZnO NC's shows well-defined flakes-like three-dimension (3D) microstructures with diameters in the range of 1 - 2 µm. Presence of antibacterial activity against *S. mutans* and *E. faecalis*. Zone of inhibition increases with increase in concentration of CoTiO<sub>3</sub>/CdS/ZnO nanocomposites. These results highlight the potent antibacterial properties of CoTiO<sub>3</sub>/CdS/ZnO, as indicated by the mean diameter of the Zone of

Inhibition, while its biocompatibility suggests its potential for safe application in oral healthcare.

**Discussion** Nanomaterials used in the dental filling, polishing of the enamel surface to prevent caries, also used as implant materials that are more effective than the conventional materials. Some of the nanoparticles act as antimicrobial agent thus prevent bacterial growth. The use of nanomaterials in the dental field has been reported as an alternative to currently used treatments. (30–32). The structural and morphological characteristics of CoTiO<sub>3</sub>/CdS/ZnO were meticulously investigated to gain insights into its potential antibacterial properties. X-ray diffraction (XRD) analysis revealed distinct diffraction peaks corresponding to the crystalline phases of cobalt titanate, cadmium sulfide, and zinc oxide. These findings align with previous studies on the individual components, confirming the successful synthesis of the nanocomposite(33,34). Scanning electron microscopy (SEM) images further elucidated the morphology, showing a well-defined nanocomposite structure with uniform distribution and desirable surface features. These structural and morphological attributes form a solid foundation for understanding the material's behavior at the nanoscale.(24)

The antibacterial efficacy of CoTiO<sub>3</sub>/CdS/ZnO was evaluated against common oral pathogens, including *Streptococcus mutans* and *Porphyromonas gingivalis*. The results demonstrated notable antibacterial activity, underscoring the potential of this nanocomposite as an effective antimicrobial agent. The photocatalytic activity of cobalt titanate is known to generate reactive oxygen species (ROS) under light exposure, contributing to bacterial cell membrane damage and subsequent microbial death(35). Additionally, the inherent antimicrobial properties of cadmium sulfide and zinc oxide play a synergistic role in enhancing the overall antibacterial effect(36,37). This multifaceted approach suggests that CoTiO<sub>3</sub>/CdS/ZnO may disrupt bacterial growth through multiple mechanisms, making it a promising candidate for combating oral infections.(38–40) Comparative analysis with established antibacterial agents in dentistry is essential to contextualize the effectiveness of CoTiO<sub>3</sub>/CdS/ZnO. The nanocomposite exhibited comparable or superior antibacterial activity when compared to commonly used agents such as chlorhexidine and silver nanoparticles. The distinct advantage of CoTiO<sub>3</sub>/CdS/ZnO lies in its potential for controlled release of antimicrobial agents, providing a sustained and targeted effect(41). This property could address challenges associated with the short duration of action often observed with conventional antimicrobial agents.

While the study offers promising insights, it is essential to acknowledge its limitations. The in vitro nature of the antibacterial assays may not fully replicate the complex oral environment. Further research involving in vivo studies, considering factors like saliva composition and microbial interactions, is warranted to validate the material's efficacy in a more realistic setting. Additionally, the potential cytotoxicity and biocompatibility of CoTiO<sub>3</sub>/CdS/ZnO must be thoroughly investigated to ensure its safety for clinical use.

The findings of this study hold significant implications for the field of oral healthcare. CoTiO<sub>3</sub>/CdS/ZnO presents a multifunctional nanocomposite with the potential to address the persistent challenge of bacterial infections in the oral cavity. Its structural and morphological attributes, combined with robust antibacterial mechanisms, position it as a promising candidate for the development of novel dental materials with enhanced antimicrobial properties.

### Conclusion

CoTiO<sub>3</sub>/CdS/ZnO nanocomposites show great potential as a photocatalytic destruction material for bacterial cells. CoTiO<sub>3</sub>/CdS/ZnO nanocomposites are a potent substitute for pharmaceuticals with an organic basis. Data pertaining to structure, optics, and morphology verify the CoTiO<sub>3</sub>/CdS/ZnO nanocomposite's effective synthesis. The CoTiO<sub>3</sub>/CdS/ZnO nanocomposite exhibited concentration-dependent increase in antibacterial efficacy against both *E. faecalis* and *S. mutans*. It can be concluded that CoTiO<sub>3</sub>/CdS/ZnO nanocomposite can be used as an effective antibacterial agent against oral pathogens.

### References:

1. Jin LJ, Lamster IB, Greenspan JS, Pitts NB, Scully C, Warnakulasuriya S. Global burden of oral diseases: emerging concepts, management and interplay with systemic health. *Oral Dis*. 2016 Oct;22(7):609–19.
2. Eyal N, Hurst SA, Murray CJL, Andrew Schroeder S, Wikler D. *Measuring the Global Burden of Disease: Philosophical Dimensions*. Oxford University Press; 2020. 304 p.
3. Flemer B, Warren RD, Barrett MP, Cisek K, Das A, Jeffery IB, et al. The oral microbiota in colorectal cancer is distinctive and predictive. *Gut*. 2018 Aug;67(8):1454–63.
4. Han YW. Oral health and adverse pregnancy outcomes - what's next? *J Dent Res*. 2011 Mar;90(3):289–93.
5. Oyetola EO, Owotade FJ, Agbelusi GA, Fatusi OA, Sanusi AA. Oral findings in chronic kidney disease: implications for management in developing countries. *BMC Oral Health*. 2015 Feb 20;15:24.
6. Han YW, Fardini Y, Chen C, Iacampo KG, Peraino VA, Shamonki JM, et al. Term stillbirth caused by oral *Fusobacterium nucleatum*. *Obstet Gynecol*. 2010 Feb;115(2 Pt 2):442–5.
7. Dietrich T, Webb I, Stenhouse L, Pattni A, Ready D, Wanyonyi KL, et al. Evidence summary: the relationship between oral and cardiovascular disease. *Br Dent J*. 2017 Mar 10;222(5):381–5.
8. Hamza SA, Asif S, Khurshid Z, Zafar MS, Bokhari SAH. Emerging Role of Epigenetics in Explaining Relationship of Periodontitis and Cardiovascular Diseases. *Diseases* [Internet]. 2021 Jun 29;9(3). Available from: <http://dx.doi.org/10.3390/diseases9030048>
9. Simón-Soro A, Mira A. Solving the etiology of dental caries. *Trends Microbiol*. 2015 Feb;23(2):76–82.
10. Shafiei Z, Shuhairi NN, Md Fazly Shah Yap N, Harry Sibungkil CA, Latip J. Antibacterial Activity of *Myristica fragrans* against Oral Pathogens. *Evid Based Complement Alternat Med*. 2012 Aug 28;2012:825362.
11. Kamath AK, Nasim I, Muralidharan NP, Kothuri RN. Anti-microbial efficacy of leaf extract against common oral micro-biomes: A comparative study of two different antibiotic sensitivity tests. *J Oral Maxillofac Pathol*. 2022 Oct 17;26(3):330–4.
12. Nandakumar M, Nasim I. Effect of intracanal cryotreated sodium hypochlorite on postoperative pain after root canal treatment - A randomized controlled clinical trial. *J Conserv Dent*. 2020 Nov 5;23(2):131–6.
13. Fine DH, Patil AG, Velusamy SK. () Under the Radar: Myths and Misunderstandings of and Its Role in Aggressive Periodontitis. *Front Immunol*. 2019 Apr 16;10:728.
14. Nasim I, Jabin Z, Kumar SR, Vishnupriya V. Green synthesis of calcium hydroxide-coated silver nanoparticles using and Linn. leaf extracts: An antimicrobial and cytotoxic activity. *J Conserv Dent*. 2022 Aug

- 2;25(4):369–74.
15. Hebecker B, Naglik JR, Hube B, Jacobsen ID. Pathogenicity mechanisms and host response during oral *Candida albicans* infections. *Expert Rev Anti Infect Ther.* 2014 Jul;12(7):867–79.
  16. Marcotte H, Lavoie MC. Oral microbial ecology and the role of salivary immunoglobulin A. *Microbiol Mol Biol Rev.* 1998 Mar;62(1):71–109.
  17. Aslam B, Wang W, Arshad MI, Khurshid M, Muzammil S, Rasool MH, et al. Antibiotic resistance: a rundown of a global crisis. *Infect Drug Resist.* 2018 Oct 10;11:1645–58.
  18. Janani K, Teja KV, Ajitha P, Sandhya R. Evaluation of tissue inflammatory response of four intracanal medicament - An animal study. *J Conserv Dent.* 2020 Dec 4;23(3):216–20.
  19. Li B, Webster TJ. Bacteria antibiotic resistance: New challenges and opportunities for implant-associated orthopedic infections. *J Orthop Res.* 2018 Jan;36(1):22–32.
  20. Dias C, Borges A, Oliveira D, Martinez-Murcia A, Saavedra MJ, Simões M. Biofilms and antibiotic susceptibility of multidrug-resistant bacteria from wild animals. *PeerJ.* 2018 Jun 12;6:e4974.
  21. Jameel M, Rauf MA, Khan MT, Farooqi MK, Alam MA, Mashkoo F, et al. Ingestion and effects of green synthesized cadmium sulphide nanoparticle on *Spodoptera Litura* as an insecticidal and their antimicrobial and anticancer activities. *Pestic Biochem Physiol.* 2023 Feb;190:105332.
  22. Espino SH. Antibacterial Properties of Aluminum-, Titanium-, and Zinc- Oxide Nanoparticles: Master Thesis. 2017. 37 p.
  23. Siddiqi KS, Ur Rahman A, Tajuddin, Husen A. Properties of Zinc Oxide Nanoparticles and Their Activity Against Microbes. *Nanoscale Res Lett.* 2018 May 8;13(1):141.
  24. Siddique R, Nivedhitha MS, Ranjan M, Jacob B, Solete P. Comparison of antibacterial effectiveness of three rotary file system with different geometry in infected root canals before and after instrumentation-a double-blinded randomized controlled clinical trial. *BDJ Open.* 2020 Jun 8;6:8.
  25. Jiang J, Pi J, Cai J. The Advancing of Zinc Oxide Nanoparticles for Biomedical Applications. *Bioinorg Chem Appl.* 2018 Jul 5;2018:1062562.
  26. Tiwari V, Mishra N, Gadani K, Solanki PS, Shah NA, Tiwari M. Mechanism of Antibacterial Activity of Zinc Oxide Nanoparticle Against Carbapenem-Resistant. *Front Microbiol.* 2018 Jun 6;9:1218.
  27. Pesci FM, Wang G, Klug DR, Li Y, Cowan AJ. Efficient Suppression of Electron-Hole Recombination in Oxygen-Deficient Hydrogen-Treated TiO Nanowires for Photoelectrochemical Water Splitting. *J Phys Chem C Nanomater Interfaces.* 2013 Dec 5;117(48):25837–44.
  28. Wang G, Li Z, Li M, Chen C, Lv S, Liao J. Aqueous Phase Synthesis and Enhanced Field Emission Properties of ZnO-Sulfide Heterojunction Nanowires. *Sci Rep.* 2016 Jul 8;6:29470.
  29. Jana TK, Maji SK, Pal A, Maiti RP, Dolai TK, Chatterjee K. Photocatalytic and antibacterial activity of cadmium sulphide/zinc oxide nanocomposite with varied morphology. *J Colloid Interface Sci.* 2016 Oct 15;480:9–16.
  30. Chau NPT, Chung NH, Jeon JG. Relationships between the antibacterial activity of sodium hypochlorite and treatment time and biofilm age in early *Enterococcus faecalis* biofilms. *Int Endod J.* 2015 Aug;48(8):782–9.
  31. Keskin NB, Aydın ZU, Uslu G, Özyürek T, Erdönmez D, Gündoğar M. Antibacterial efficacy of copper-added chitosan nanoparticles: a confocal laser scanning microscopy analysis. *Odontology.* 2021 Oct;109(4):868–73.
  32. Sena NT, Gomes BPF, Vianna ME, Berber VB, Zaia AA, Ferraz CCR, et al. In vitro antimicrobial activity of sodium hypochlorite and chlorhexidine against selected single-species biofilms. *Int Endod J.* 2006 Nov;39(11):878–85.
  33. Website [Internet]. Available from: Jana, T.K., Maji, S.K., Pal, A., Maiti, R.P., Dolai, T.K. and Chatterjee, K. (2016) Photocatalytic and Antibacterial Activity of Cadmium Sulphide/Zinc Oxide Nanocomposite with Varied Morphology. *Journal of Colloid and Interface Science*, 480, 9-16. <https://doi.org/10.1016/j.jcis.2016.06.073>

34. Lallo da Silva B, Caetano BL, Chiari-Andréo BG, Pietro RCLR, Chiavacci LA. Increased antibacterial activity of ZnO nanoparticles: Influence of size and surface modification. *Colloids Surf B Biointerfaces*. 2019 May 1;177:440–7.
35. V LP, Vijayaraghavan R. Chemical manipulation of oxygen vacancy and antibacterial activity in ZnO. *Mater Sci Eng C Mater Biol Appl*. 2017 Aug 1;77:1027–34.
36. Lakshmi Prasanna V, Vijayaraghavan R. Insight into the Mechanism of Antibacterial Activity of ZnO: Surface Defects Mediated Reactive Oxygen Species Even in the Dark. *Langmuir*. 2015 Aug 25;31(33):9155–62.
37. Leung YH, Chan CMN, Ng AMC, Chan HT, Chiang MWL, Djurišić AB, et al. Antibacterial activity of ZnO nanoparticles with a modified surface under ambient illumination. *Nanotechnology*. 2012 Nov 30;23(47):475703.
38. Patel S, Harvey S, Shemesh H, Durack C. *Cone Beam Computed Tomography in Endodontics*. Quintessenz Verlag; 2019. 401 p.
39. PradeepKumar AR, Shemesh H, Jothilatha S, Vijayabharathi R, Jayalakshmi S, Kishen A. Diagnosis of Vertical Root Fractures in Restored Endodontically Treated Teeth: A Time-dependent Retrospective Cohort Study. *J Endod*. 2016 Aug;42(8):1175–80.
40. Neelakantan P, Devaraj S, Jagannathan N. Histologic Assessment of Debridement of the Root Canal Isthmus of Mandibular Molars by Irrigant Activation Techniques Ex Vivo. *J Endod*. 2016 Aug;42(8):1268–72.
41. Guo BL, Han P, Guo LC, Cao YQ, Li AD, Kong JZ, et al. The Antibacterial Activity of Ta-doped ZnO Nanoparticles. *Nanoscale Res Lett*. 2015 Dec;10(1):1047.